Polymer Chemistry



PAPER View Article Online
View Journal | View Issue



Cite this: *Polym. Chem.*, 2023, **14**, 1054

Received 3rd November 2022, Accepted 31st January 2023 DOI: 10.1039/d2py01389d

rsc.li/polymers

PET-RAFT to expand the surface-modification chemistry of melt coextruded nanofibers†

Justin D. Hochberg, David M. Wirth Dand Jonathan K. Pokorski D*

Polymeric nanofibers have been widely used as scaffolds for tissue engineering, drug delivery, and filtration applications, among many others. A high throughput melt coextrusion technique and post-processing functionalization chemistry was recently developed to fabricate functional fibers with nanoscale dimensions. This manuscript expands upon the development of nanofiber modification chemistry by functionalizing fiber mats using a surface-initiated photo-induced electron transfer reversible addition–fragmentation chain transfer (PET-RAFT) polymerization technique. PET-RAFT allows for the fabrication of chemically diverse nanofiber systems initiated with light, preventing the need for high temperature thermal initiators. This manuscript describes the scope of monomers polymerizable *via* this technique on the surface of poly ε-caprolactone (PCL) nanofibers. The PET-RAFT modification chemistry is used to introduce block copolymers, provide multiple modifications using an orthogonal RAFT-ATRP system, induce spatial photopatterning and to establish cell-adhesive capabilities. The development of surface-initiated PET-RAFT adds an additional tool to a growing strategy for nanofiber functionalization.

1. Introduction

Polymeric nanofiber materials have applications in a variety of fields including filtration,1 energy storage,2 and especially for use in various areas of biomedicine³ including wound healing,4 drug delivery,5 and tissue engineering.6,7 The most common method to fabricate nanofibers is electrospinning because it is inexpensive, simple to run, and can provide excellent control of nanofiber dimensions.^{3,8} While electrospinning has been effectively used in a variety of research environments, it has a low maximum throughput, even when using commercial instrumentation,9 and the size and quality of the fabricated nanofibers are heavily dependent on environmental conditions. 10,11 These downfalls significantly inhibit the commercial translation of the electrospinning technique. Newer techniques exist, but many also feature innate limitations. Melt electrospinning is a similar technique that requires higher voltages while providing a lower throughput than conventional solvent-based electrospinning;12 melt blowing has difficulty producing nanoscale fibers;¹³ and rotary jet spinning produces fibers with weak mechanical properties. 14,15 Melt coextrusion has emerged recently for nanofiber fabrication and is a method that produces nanoscale fibers at scale, is

Department of NanoEngineering, University of California San Diego, Jacobs School of Engineering, 9500 Gilman Dr, SME Building 243J, La Jolla, California 92093, USA. E-mail: jpokorski@ucsd.edu; Tel: +858-246-3183

†Electronic supplementary information (ESI) available. See DOI: https://doi.org/ 10.1039/d2py01389d solvent-free, and can fabricate nanofibers with robust mechanical properties. In addition the throughput is exceptionally high, generating fibers at a rate of 2 kg $\rm h^{-1}$ when applied using a laboratory scale extruder. $^{16-18}$

In principle, most thermoplastic polymers can be used during fiber coextrusion, however we chose to use polyesters due to their utility in biomedical applications. Polyesters are known to have useful and tunable mechanical properties, can be easily modified, and are a workhorse class of polymers for melt extrusion. Poly(ϵ -caprolactone) (PCL) has been heavily utilized during melt co-extrusion yielding fibers with a slow hydrolytic degradation rate, high ductility, and providing nanofibers able to reach more than 700% elongation at break. 19,20

Native PCL nanofibers have limited uses because the surface of the fibers is especially hydrophobic and provides no appreciable chemical or biochemical signaling that would be useful for advanced applications, such as those in the biomedical arena. While unmodified nanofibers have useful physical and mechanical properties, they must be chemically modified to introduce functional properties.²¹ To widen the breadth of applications of polymeric nanofibers, functional moieties can be introduced to the nanofiber surface. Various methods exist to introduce functionality onto polyesters include hydrolysis,²² aminolysis,²³ end group modification,²⁴ and photochemical covalent insertion.²⁵ Chemical modification of polyester nanofibers has led to the formation of useful materials including those promoting antibacterial,⁴ antifouling,²⁶ and tissue engineering properties.^{6,8,17}

This manuscript describes the fabrication of functional nanofiber mats *via* a surface initiated photoinduced electron transfer reversible addition–fragmentation chain transfer polymerization (PET-RAFT) mechanism using air-tolerant conditions. PET-RAFT is a light-initiated controlled radical polymerization technique that is a simple method for nanofiber functionalization, which allows for the fabrication of nanofibers with a wide range of chemical functionalities.^{27–29} PET-RAFT can be conducted under ambient conditions without the need for rigorous degassing of the reaction solution. Additionally, the mechanism for PET-RAFT is orthogonal to other polymerization chemistries, such as atom-transfer radical polymerization (ATRP), allowing for the generation of multifunctional materials.

2. Materials and methods

2.1. Materials

Polyethylene Oxide (PEO) POLYOX N10 (100 kDa) and POLYOX N80 (200 kDa) were both purchased from Dow Chemical while CAPA 6800 PCL-80 kDa was purchased from the Perstorp Group. 4-Cyano-4-(dodecylsulfanylthiocarbonyl)sulfanylpentapurchased from Strem Chemicals. was 4-Hydroxybenzophenone was purchased from Acros Organics. N,N'-Dicyclohexylcarbodiimide (DCC), Dimethylaminopyridine (DMAP), acrylic acid, poly(ethylene glycol) (PEG) methacrylate $(M_{\rm n}=360~{\rm g~mol^{-1}})$, fluorescein *o*-acrylate, 9-anthracenylmethyl acrylate, copper(1) bromide, and α-bromoisobutyryl bromide were purchased from Sigma-Aldrich. Methacrylic Acid was purchased from TCI America. Dimethylacrylamide (DMA), N-isopropylacrylamide (NIPAM), 9,10-dimethylanthracene zinc meso-tetraphenylporphine (ZnTPP), Dulbecco's Modified Eagle's medium (DMEM), and Detachin were purchased from Fisher Scientific. Methacryloxyethyl thiocarbamoyl rhodamine B was purchased from Polysciences. GRGDS-acrylate was purchased from GenScript. 1-Bromohexane and tris(2-dimethylaminoethyl)amine (Me6TREN) were purchased from Alfa Aesar. Phosphate buffered saline (PBS) pH 7.4 1× and penicillin-streptomycin (5000 U mL⁻¹) were purchased from Gibco. Fetalgro Bovine Growth Serum was purchased from RMBio. NIH3T3 cell line was purchased from ATCC.

2.2. Instrumentation and equipment

PEO was compounded in a Haake Rheodrive 5000 twin-screw extruder. Melt coextrusion was conducted on a custom, two-component system consisting of a series of vertical and horizontal multipliers. A SereneLifeSLPRWAS26 Compact Pressure Washer (1500 psi maximum pressure, 3 mm length by 11 mm width) was used to wash away excess PEO and entangle isolated nanofibers into mats. An Anytime Tools sharp 1/4" hollow punch was used to shape nanofiber mats into circular patches. An Omnicure Model S1500 standard filter 320–500 nm UV light source was used for photo-chemical modification with benzophenone derivatives. A FEI Apreo LoVac FESEM was used for taking electron micrographs.

Nuclear magnetic resonance data was obtained with a 300 MHz Bruker Avance III spectrometer. A custom-built light box (λ = 650 nm) was used for RAFT photochemistry. Water contact angle images were obtained with a ramé hart Model 200 goniometer. X-ray photoelectron spectroscopy data was obtained with a Kratos Analytical AXIS Supra surface analysis instrument. An Invitrogen EVOS FL Digital Inverted Fluorescence Microscope was used for fluorescent images. UV fluorescent mats were excited with a UVP UVGL-15 Compact UV Lamp (254/365 nm. 4 W, 0.16 A, 115 V, 60 Hz). Photographs of UV-patterned mats were taken with a Sony RX100 IV 20.1 MP Digital Camera. Confocal images were taken with a Leica SP8 Laser Confocal Microscope.

2.2.1. Melt coextrusion of PCL/PEO compound tapes. Two different molecular weights of PEO (100 kDa and 200 kDa) were first dried in a vacuum oven at 40 °C for 48 hours, then compounded in a twin-screw extruder (140 °C) at a 70/30 w/w% ratio to provide a rheological match to PCL at the extrusion temperature. Following compounding, the PEO and PCL pellets were dried for an additional 48 hours at 40 °C. PEO and PCL were then coextruded at 180 °C on an extrusion line consisting of 16 vertical and 4 horizontal multipliers with a 33% by volume PEO skin layer. The finished composite tape then exited through a 3" tape die and was collected on a chill roll rotating at 15 rpm at room temperature. 26

2.2.2. Nanofiber isolation and formation of PCL mats. Composite PEO/PCL tapes were first secured in a beaker of stirring water for 6 hours; water was changed hourly. The tapes were then immersed in a 70% MeOH solution overnight, revealing PCL nanofibers. The nanofibers were subsequently secured to a fiberglass plate in a single layer and covered with a wire mesh to be washed with a pressure washer with varying spray sizes. The nonwoven nanofiber mats were then dried overnight in a vacuum desiccator before being punched out into 6 mm circular patches.

2.2.3. Synthesis of nanofiber inserting RAFT CTA (benz-4-Cyano-4-(dodecylsulfanylthiocarbonyl)sulfanylpentanoic acid (0.810 g, 2.007 mmol), N,N'-dicyclohexylcarbodiimide (DCC) (0.497 g, 2.407 mmol), and 4-dimethylaminopyridine (DMAP) (0.078 g, 0.030 mmol) were dissolved in 20 mL of dichloromethane (DCM) and stirred for 30 minutes at 0 °C to activate the carboxylic acid. 4-Hydroxybenzophenone (0.398 g, 2.007 mmol) was dissolved in 10 mL of DCM and added dropwise to the reaction mixture. The ice bath was replaced, and the reaction was left to reach room temperature and proceed overnight. The reaction mixture was then placed at 4 °C for 20 minutes to allow dicyclohexylurea to fully precipitate before being filtered off and the crude product concentrated in vacuo. The crude product was then redissolved in a small amount of DCM and washed twice with sodium bicarbonate, and three times with water. The organic layer was dried over anhydrous sodium sulfate and concentrated in vacuo. The crude product was purified via column chromatography with 25% ethyl acetate and 75% hexane. Once the product was collected, it was once again concentrated in vacuo to yield a sticky yellow solid. Yield: (0.853 g, 1.456 mmol, 72.8%) ¹H NMR (300 MHz,

Paper

CDCl₃), δ (ppm): 7.86 (2H, dt), 7.79 (2H, dt), 7.60 (1H, tt), 7.50 (1H, tt), 7.24 (2H, dt), 3.35 (2H, t), 2.94 (2H, t), 2.59 (2H, m), 1.95 (3H, s), 1.71 (2H, quint), 1.40 (2H, quint) 1.26 (16H, s), 0.88 (3H, t).

2.2.4. Nanofiber functionalization with RAFT benz-CTA. Nonwoven nanofiber mats (6 mm diameter, \sim 4.5 mg) were added to a 7.5 mg mL⁻¹ solution of benz-CTA in MeOH and then placed in a vacuum desiccator and dried overnight. The mats were then placed underneath a broadband UV lamp (λ = 320–500 nm, 548 mW cm⁻²) for 35 minutes per side. Functionalized mats were washed three times with MeOH and dried overnight in a vacuum desiccator. CTA functionalization was confirmed via water contact angle (WCA) and X-ray photoelectron spectroscopy (XPS).

2.2.5. Surface initiated PET-RAFT. CTA-functionalized mats, monomer (1.388 mmol), ZnTPP (0.05 mg, 47 μ L of 1 mg mL⁻¹ solution, 0.069 μ mol), 9,10-dimethylanthracene (1.57 mg, 0.008 mmol), and benz-CTA (4.05 mg, 0.007 mmol) were added to 2 mL of DMSO in a 20 mL scintillation vial and placed under red light (λ = 650 nm, 81 mW cm⁻²) for 3 hours. Mats were then washed three times in MeOH and dried in a vacuum desiccator overnight. Polymer functionalization was confirmed νia WCA and XPS.

2.2.6. Preparation of fluorescently labeled nanofiber mats

2.2.6.1. Preparation of block copolymer mats. To graft block copolymers from the nanofiber surface, procedure 2.2.5 was conducted twice. The first time utilizing 99% acrylic acid (99 mg, 1.374 mmol) and 1% fluorescein o-acrylate (5.3 mg, 0.014 mmol) as the monomers, and the second time utilizing 99% acrylic acid (99.0 mg, 1.374 mmol) and 1% methacryloxyethyl thiocarbamoyl rhodamine B (8.9 mg, 0.014 mmol) as the monomers. Polymer functionalized nanofiber mats were washed three times in MeOH and vacuum dried overnight. Polymer functionalization was confirmed via WCA and XPS and mats were then imaged under the FITC and Texas Red settings of a fluorescent microscope.

2.2.6.2. Preparation of orthogonal RAFT/ATRP Following CTA functionalization in Section 2.2.4, nanofiber mats were then incubated with a similar benz-ATRP initiator in 10 mg mL⁻¹ in MeOH whose synthesis has been described previously.4 Saturated mats were once again placed underneath a broadband UV lamp ($\lambda = 320-500 \text{ nm}$, 548 mW cm⁻²) for 35 minutes per side, washed three times with methanol, then dried overnight in a vacuum desiccator. PET-RAFT was then conducted as described in section 2.2.5, with 99% acrylic acid (99 mg, 1.374 mmol) and 1% fluorescein o-acrylate (5.3 mg, 0.014 mmol) as the monomers. Polymer functionalized mats were then washed three times with MeOH and dried overnight in a vacuum desiccator. Surface initiated atom transfer radical polymerization (SI-ATRP) was then conducted off the nanofibers. Acrylic acid/fluorescein o-acrylate modified mats, 99% acrylic acid (99.0 mg, 1.374 mmol) and 1% methacryloxyethyl thiocarbamoyl rhodamine B (8.9 mg, 0.014 mmol) as the monomers, Me₆TREN, and dimethylformamide (2 mL) were added to a three-neck round bottom flask and bubbled with N_2 gas for 50 minutes. Cu(1)Br (4.0 mg, 0.028 mmol) was then

added under positive pressure. The reaction was allowed to proceed overnight at room temperature. The orthogonally modified mats were then washed three times with MeOH and dried in a vacuum desiccator. Polymer functionalization was confirmed *via* WCA and XPS and mats were then imaged under the FITC and Texas Red settings of a fluorescent microscope.

2.2.7. Preparation of patterned, UV fluorescent nanofiber mats. Unmodified PCL mats were functionalized as describe in section 2.2.4 with a photomask displaying "UCSD" on top. PET-RAFT was conducted as described in section 2.2.5, with 99% acrylic acid (99 mg, 1.374 mmol) and 1% 9-anthracenylmethyl acrylate (3.6 mg, 0.014 mmol) as the monomers. Polymer functionalized mats were then washed three times with MeOH and dried overnight in a vacuum desiccator. A handheld UV lamp (λ = 365 nm, 0.16 A) and a photograph was taken.

2.2.8. Preparation of cell adhesion peptide modified nanofiber mats. PET-RAFT was conducted as described in section 2.2.5, with 99% PEG methacrylate (493 mg, 1.374 mmol) and 1% GRGDS acrylate (7.6 mg, 0.014 mmol). Polymer mats were also prepared with 100% PEG methacrylate (500 mg, 1.388 mmol) as a control. Polymer functionalized mats were then washed three times with MeOH and dried overnight in a vacuum desiccator. Polymer functionalization was confirmed via WCA and XPS.

2.2.9. Patterning of cell adhesion peptide modified mats. Mouse fibroblasts (NIH3T3) were cultured in a T75 tissue culture flask in DMEM supplemented with 10% by volume FetalGro serum, 1% by volume L-glutamine, and 1% by volume 5000 U mL⁻¹ penicillin-streptomycin. Cells were grown to 85% confluence in an environment with 5% CO2 and a relative humidity of 95%, then washed with 5 mL of PBS and trypsinized with 5 mL of Detachin for 5 minutes. Cells were then washed with PBS and centrifuged before being stained with 0.1 μg mL⁻¹ Hoechst 33342 in media without serum. The cells were then washed and centrifuged three more times with PBS before being redissolved in 1 mL of media and counted with a hemocytometer. PEG methacrylate/GRGDS, 100% PEG methacrylate, and unmodified nanofiber mats were then placed in individual sections of a 4-section glass bottom Petri dishes and covered with 0.5 mL of 625 cells per mm². Cells adhered to the nanofiber mats were then imaged with confocal microscopy using the DAPI setting.

3. Results and discussion

3.1. Melt coextrusion of PCL/PEO compound tapes

In this work composite tapes comprised of PCL nanofibers embedded within a sacrificial PEO matrix were fabricated. PCL is chosen as the nanofiber material due to the ability for post-extrusion modification, biocompatibility, and ductility. PEO is used as a sacrificial coextrudate because blending of different molecular weights results in an immiscible rheological match to PCL, leading to distinct layering during extrusion. In

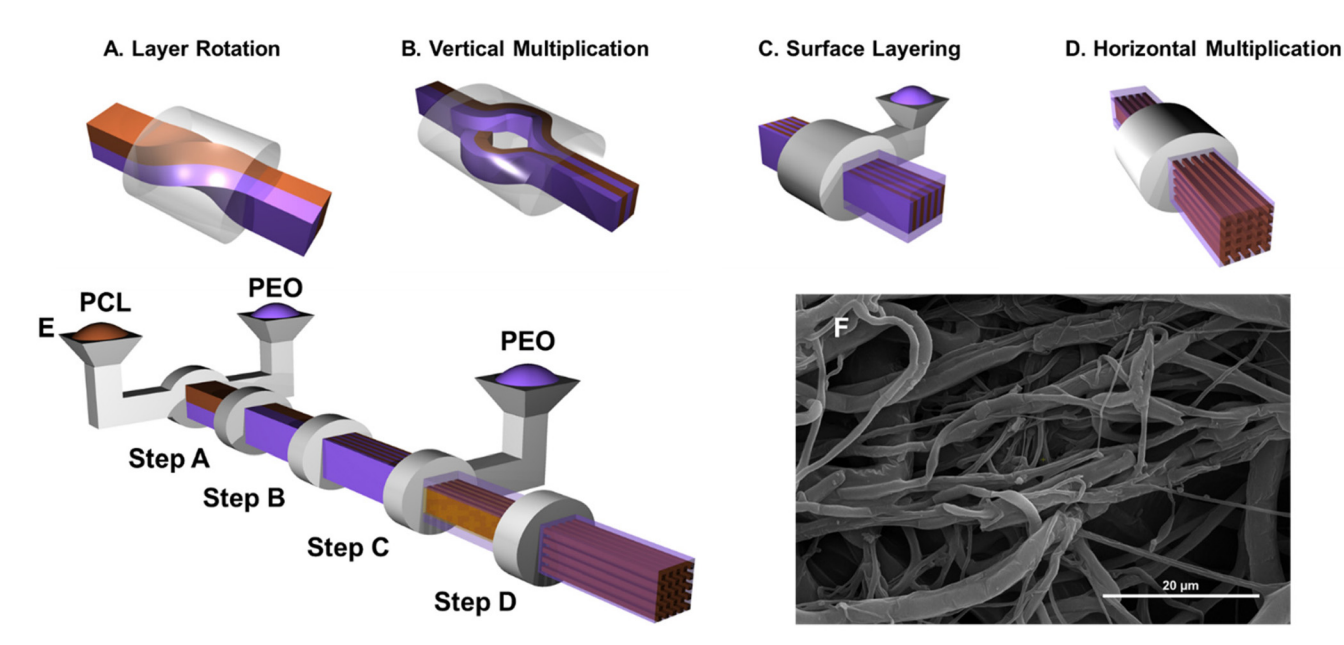


Fig. 1 (A–E) Schematic diagram of melt coextrusion system describing steps within the extrusion line (A) layer rotation, (B) vertical multiplication, (C) surface layering, (D) horizontal multiplication procedures, and (E) overview of system. (F) Scanning electron micrograph of extruded and isolated nanofibers (scale bar = 20 μm).

addition, PEO is water soluble allowing for a simple aqueous dissolution of the sacrificial material to reveal nanofibers. PCL and PEO are coextruded by individually melt-pumping the two polymers in vertically oriented layers in the extrusion line. The layers are then rotated 90° to orient the polymer melts to flow side-byside (Fig. 1A). The melt flow is then fed into a series of vertical multipliers, which effectively double the number of layers, thus creating a total of 2^{n+1} total vertical layers, where "n" is the number of vertical multipliers (Fig. 1B). A 33% skin layer of PEO then covers the top and bottom of the polymer melt (Fig. 1C). Lastly, a series of horizontal multipliers yields the nanoscopic PCL domains embedded inside of the PEO matrix after the melt exits the set-up through a 3" tape die (Fig. 1D). This entire process (Fig. 1E) yields 2^m horizontal layers and 2^{n-m} vertical layers, where "m" is the number of horizontal multipliers. This work used 16 vertical and 4 horizontal layers, resulting in 4096 × 16 PCL nanofiber domains within the PEO matrix (Fig. 1F).

3.2. Formation of PCL nanofiber mats

PCL nanofibers are embedded in a PEO matrix within a composite tape in the extrudate. Composite tapes were washed in a stirring water bath for 6 hours, with the water being replaced every hour. The water bath step is followed by a 70% MeOH bath overnight. Nanofibers are then sprayed with a high-pressure water jet to remove any remaining PEO. This water jetting step yields nanofibers with a 97% PEO removal as determined by NMR (Fig. S1†). Nanofiber mats are then punched into a disc shape with a diameter of 6 mm.

3.3. Functionalization of nanofiber mats with RAFT CTA

A RAFT chain transfer agent (CTA) was conjugated to the PCL backbone of the nanofibers to graft polymers off the surface of

the nanofiber mats (Fig. 2A). A CTA-modified benzophenone was first synthesized (Fig. S2†) *via* a Steglich Esterification³¹ prior to nanofiber insertion. Under UV light, benzophenone is known to undergo a hydrogen abstraction which allows insertion of the molecule into the PCL backbone.²⁵ We aimed to take advantage of this mechanism for the insertion of our CTA-modified benzophenone molecule into the PCL chains of our nanofiber mats. The mats were first dip-coated in a solution containing the benzophenone-CTA, subsequently dried under vacuum, then illuminated under UV light to initiate the photochemical insertion. This process yielded nanofibers functionalized with a RAFT CTA ready to undergo further functionalization. CTA-modified fibers were characterized *via* WCA and XPS, demonstrating an increased contact angle and noticeable sulfur signal, respectively (Fig. 3).

3.4. Grafting-from PET-RAFT

PET-RAFT was conducted from the CTA-modified nanofiber mats using red light to initiate the polymerization (Fig. 2A). Our goal was to further develop and expand on the chemistries used to create functional nanofiber materials. One aim of this manuscript was to develop biocompatible methods to prepare functional fibers (as opposed to Cu-mediated SI-ATRP). Utilizing a visible light-based initiator instead of a thermal-based initiator allows materials to be formed at low temperatures, a necessary concern due to PCL's low melting point of ~60 °C. ^{32,33} Compared to similar ATRP methods, RAFT chemistry does not require a toxic metal catalyst such as Cu, instead obtaining its living characteristics from the CTA. ³⁴ PET-RAFT is also oxygen tolerant, allowing for polymerization in ambient conditions without the need for rigorous degassing. ²⁹

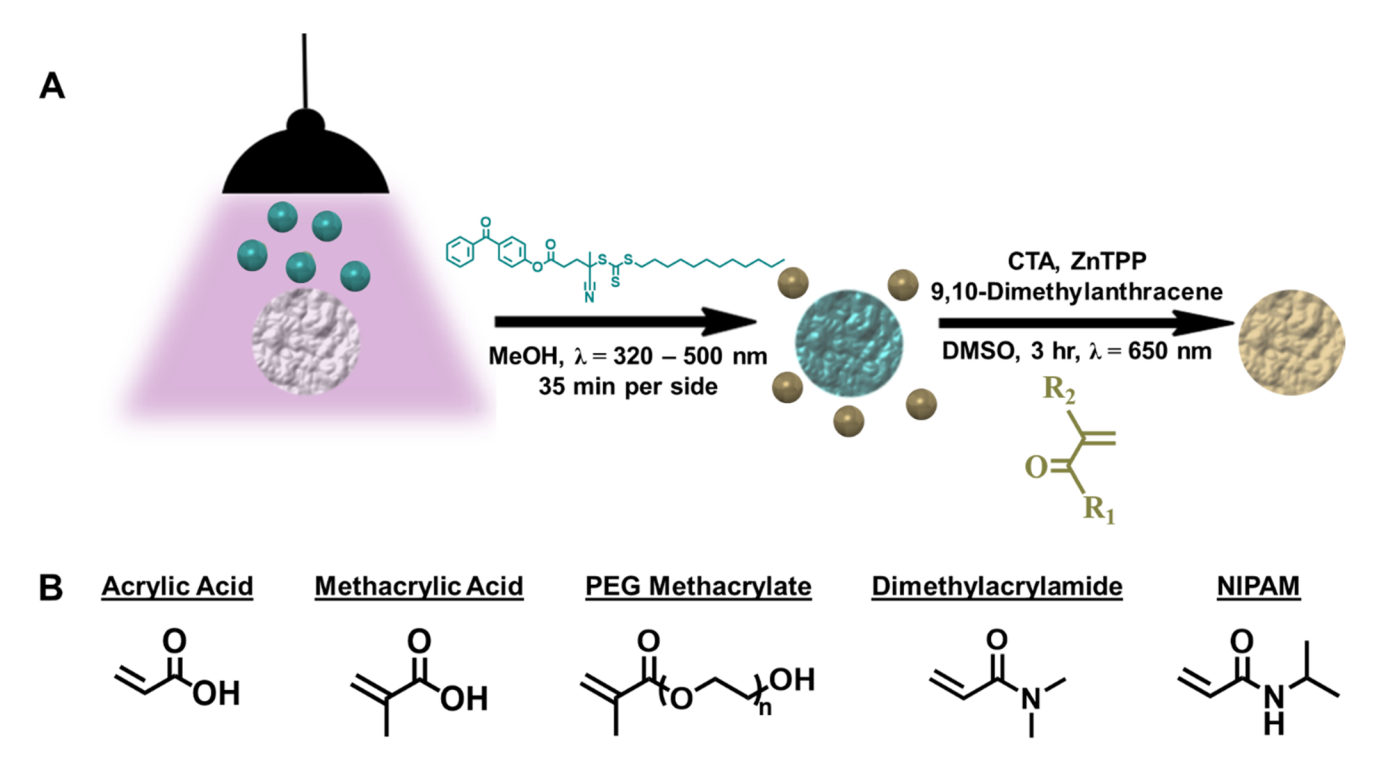


Fig. 2 Overview of PET-RAFT nanofiber functionalization including (A) reaction schematic, (B) monomers used in main functionalizations.

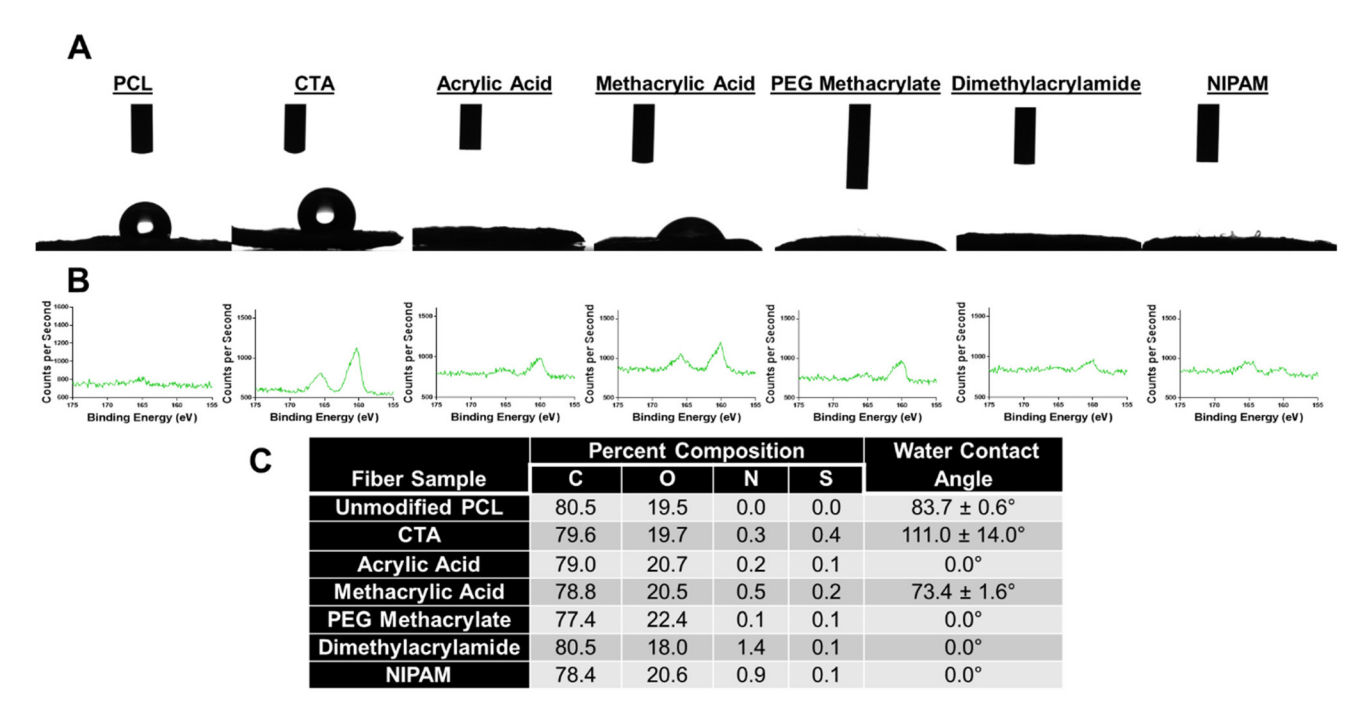


Fig. 3 Characterizations of functionalized nanofiber mats including (A) water contact angles, (B) High resolution X-ray photoelectron spectroscopy of S2p of the various nanofiber mats, and (C) an overview of the characterization data.

A library of monomers (Fig. 2B) was used to explore the breadth of chemistries possible with this technology and included acrylic acid, methacrylic acid, PEG methacrylate, dimethylacrylamide, and N-isopropyl acrylamide (NIPAM).

PET-RAFT was optimized to be carried out for 3 hours to maximize functionality while minimizing photobleaching of fluorescent components; further optimization could be carried out to modify the thickness of brushes in the future. WCA and

XPS (Fig. 3) were used to characterize the polymer modified nanofiber mats. WCA results showed a significant increase in the hydrophobicity of the PCL nanofiber mats upon modification with the benzophenone-CTA, revealing an increase in the contact angle from 83.7 \pm 0.6° to 111.0 \pm 14.0°. This increase is due to the long hydrocarbon tail of the CTA. Upon modification with the selected polymers however, the nanofiber mats become extremely hydrophilic. Mats modified with acrylic acid, PEG methacrylate, dimethylacrylamide, and NIPAM fully wet with a contact angle of 0°. Methacrylic acid mats showed increased hydrophilicity reaching a contact angle of $73.4 \pm 1.6^{\circ}$ but did not fully wet due to the additional

Upon modification with the CTA, XPS integrations show that the nanofiber mats contain a small percentage of nitrogen and sulfur, 0.3% and 0.4% respectively, and continue to show evidence of CTA throughout the polymerizations. Polymerized

nanofiber mats show further evidence of polymer modification based on changes in the distribution of individual atomic species. For instance, acrylamide modified mats all show an increase in nitrogen content and all modified mats retained sulfur from the CTA. These results show the ability of this technique to decorate the nanofiber surface with a wide variety of different functionalities.

3.5. Preparation of fluorescently labeled nanofiber mats

3.5.1. Block copolymer mats. The unique nature of the CTA modified nanofiber mats allows for the implementation of more complex chemistries since PET-RAFT is functional group tolerant. Block polymer (Fig. 4A) and orthogonally functionalized (PET-RAFT followed by ATRP) mats were prepared to demonstrate this (Fig. 4B).

To illustrate the living nature of the modified nanofiber mats, a block polymer was grafted from the nanofiber surface

A. Block Copolymers:

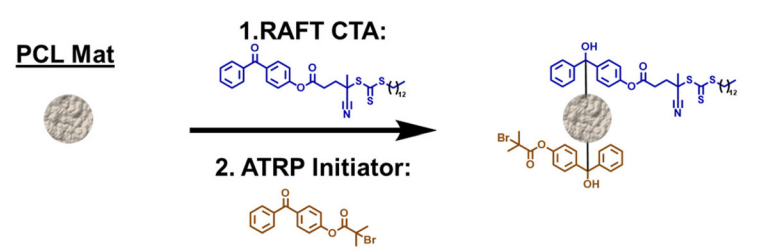
methyl group in the polymer backbone.

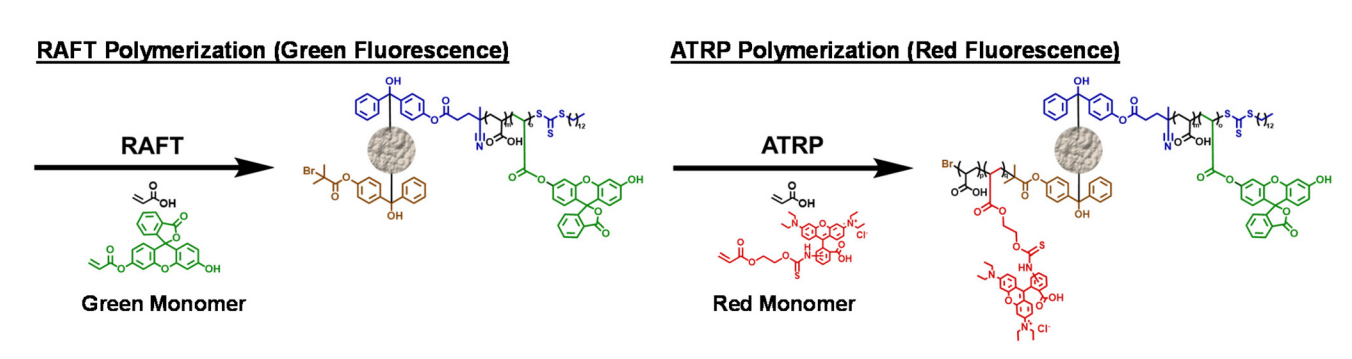
Polymer Chemistry

CTA Functionalized Mat Mat With 1 Block Mat With 2 Blocks Red Monomer **Green Monomer**

B. Orthogonal Chemistry:

UV-insertion of RAFT CTA and ATRP Initiator





Reaction scheme of (A) block copolymer modified nanofiber mats and (B) RAFT/ATRP orthogonally modified nanofiber mats.

via PET-RAFT using fluorescent monomers. Both blocks contained 99% acrylic acid with a small amount of an orthogonal fluorescent dopant. The first block was functionalized with 1% fluorescein acrylate (green) while the second block was functionalized with rhodamine B (red). RAFT block copolymer modified mats (Fig. 5C, G, and K) showed strong green and red fluorescence. This strong fluorescence in both regions indicated the successful functionalization *via* two subsequent polymerization reactions indicating block copolymer formation. Unmodified PCL mats (Fig. 5A, E, and I) showed no fluorescence and mats modified only with fluorescein acrylate *via* PET-RAFT showed solely green fluorescence.

3.5.2. Orthogonal chemistry. An analogous method to modify the nanofibers with separate colors was developed utilizing two orthogonal chemistries. A benzophenone-modified ATRP initiator was prepared and underwent photochemical insertion into the PCL backbone with the RAFT CTA. PET-RAFT was then conducted with 99% acrylic acid and 1% fluorescein acrylate to generate green-fluorescent materials. Red fluorescence was then introduced using 99% acrylic acid and 1% rhodamine B acrylate via ATRP. This once again provides nanofibers displaying both green and red fluorescence using an orthogonal chemical technique. As with the block copolymer modified mats, the RAFT/ATRP orthogonally modified mats (Fig. 5D, H, and L) showed strong green and red fluorescence, once again indicating the successful functionalization of the nanofiber mats with two subsequent reactions. It is important to note that there is the potential for side reactions in this procedure. For instance, ZnTPP has been shown to inefficiently activate C-Br bonds, while Cu-ligand species can use trithiocarbonates as poor ATRP surrogates. However, these dual reactions yielded the surface characteristics that we hoped to impart.

3.6. Preparation of UV patterned nanofiber mats

Photopatterning was conducted to further demonstrate the versatility of RAFT nanofiber mat technology. A photomask with the letters UCSD (representing University of California San Diego) was placed on a larger nanofiber mat during photoinsertion of the benzophenone-CTA into the PCL backbone. Due to this photomask placement, the CTA was spatially confined where the letters UCSD were situated. PET-RAFT was then conducted with 99% acrylic acid and 1% UV active monomer (9-anthracenylmethyl acrylate) (Fig. 6A). A handheld UV lamp was then illuminated on top of the patterned nanofiber mat and a photograph was taken (Fig. 6B) and compared with a photograph under normal overhead lights (Fig. 6C).

3.7. Cell adhesion peptide modified mats

A peptide-based monomer was used to functionalize the nanofiber mats to demonstrate further utility of this technology CTA modified nanofiber mats were functionalized with 99% PEG methacrylate and 1% GRGDS-acrylate as well as 100% PEG methacrylate as a control (Fig. 7A). The GRGDS peptide motif is well known to promote cell adhesion. 35–37

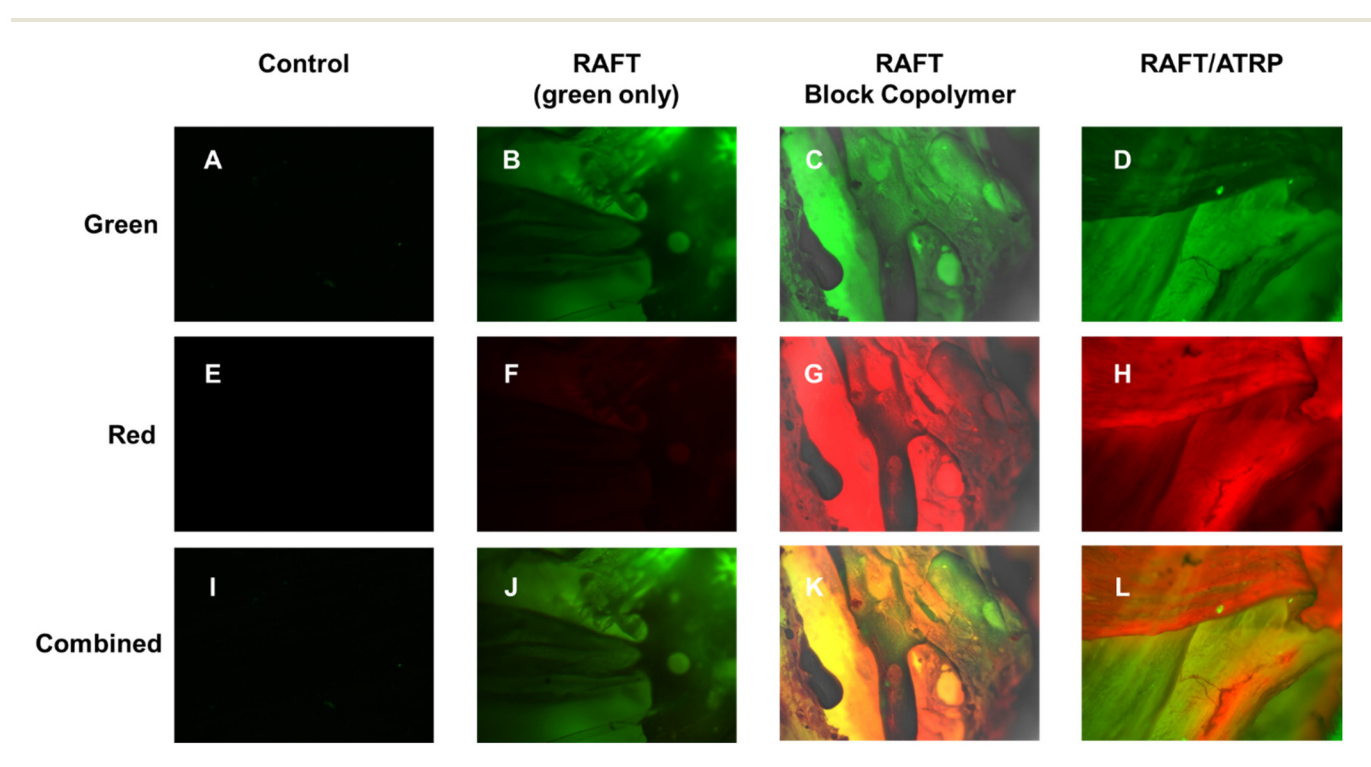


Fig. 5 Fluorescent images of nanofibers showing (A–D) green fluorescence, (E–H) red fluorescence, and (I–L) combined green and red fluorescent channels. Samples include (A, E and I) unmodified PCL nanofibers, (B, F and J) nanofibers mats only modified with the green fluorescent monomer *via* a single PET-RAFT reaction, (C, G and K) RAFT block copolymer modified nanofiber mats, and RAFT/ATRP orthogonally modified nanofiber mats (scale bar = 1 mm).

Fig. 6 (A) Chemical scheme of nanofiber mat functionalization with acrylic acid and UV active monomer. Photograph of nanofiber mat patterned with "UCSD" (B) illuminated with UV light and (C) under regular overhead lights.

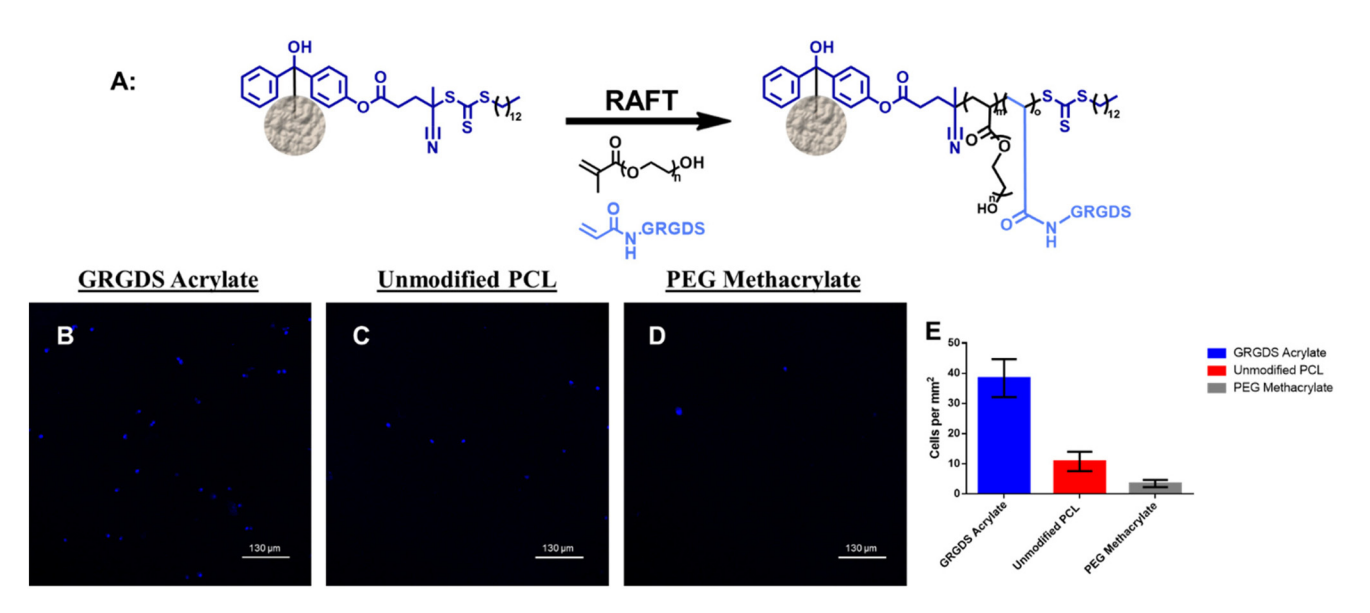


Fig. 7 (A) Chemical scheme of nanofiber mat functionalization with PEG methacrylate and GRGDS acrylate. Confocal microscopy images of cells on nanofibers (B) functionalized with GRGDS acrylate, (C) unfunctionalized, and (D) functionalized with an antifouling PEG methacrylate polymer (scale bar = 130 μ m). (E) Plot of cells on nanofiber mats per mm².

Mouse fibroblasts (NIH3T3) stained with a Hoechst dye were seeded on peptide modified mats, unmodified mats, and PEG methacrylate modified mats. PEG covered surfaces are known to possess antifouling properties, preventing cells from attaching to surfaces.²⁶ Cell seeded nanofibers were imaged

via confocal microscopy after overnight incubation (Fig. 7). Peptide-modified nanofibers (Fig. 7B) led to a cell density of 38.4 ± 6.3 cells per mm², which is nearly a 4× increase when compared with unmodified PCL mats (Fig. 7C) (10.8 \pm 3.2 cells per mm²) and a more than 10× increase when compared with

PEG methacrylate antifouling mats (Fig. 7D) (3.5 \pm 1.2 cells per mm²). These decreases in cell density (Fig. 7E) confirm that the GRGDS motif significantly increases the binding ability of cells onto the nanofiber surface, opening up these materials for tissue engineering applications in the future.

4. Conclusion

This manuscript demonstrated the successful preparation of functional nanofiber mats *via* a high-throughput melt coextrusion process followed by functionalization *via* PET-RAFT. We demonstrated the diverse utility of this technique with a library of polymers *grafted-from* the nanofiber surface as well as the ability to use complex chemistries including functionalizing with block copolymers, an orthogonal RAFT-ATRP system, photopatterning, and cell patterning capabilities. The chemistry demonstrated herein provides a platform for diverse surface functionalization of any polyester using a simple reaction setup that eliminates copper, can be performed under ambient conditions, and yields polymers with complex functional groups and architectures.

Conflicts of interest

There are no conflict to declare.

Acknowledgements

J. K. P., J. D. H., and D. M. W. acknowledge NSF Partnerships for International Research and Education (PIRE) for financial support (OISE 1844463). The authors acknowledge the use of facilities and instrumentation supported by NSF through the UC San Diego Materials Research Science and Engineering Center (UCSD MRSEC), grant # DMR-2011924. The UCSD Microscopy Core (NINDS P30NS047101) is acknowledged for confocal microscope access. Dr Xinting Wang and Dr Cong Zhang are acknowledged for the access and assistance with running the melt coextrusion system. Dr Erik Price is acknowledged for his assistance with preparations for the melt coextrusion process. Dr Dana Klein is acknowledged for assistance with the twin-screw extruder system.

References

- 1 J. Wang, M. Ponting, C. Zhang, A. Olah and E. Baer, Fuel Filtration Properties and Mechanism of a Novel Fibrous Filter Produced by a Melt-Process, *J. Membr. Sci.*, 2017, **526**, 229–241, DOI: **10.1016/j.memsci.2016.12.040**.
- 2 S. Nagata, G. M. Atkinson, D. Pestov, G. C. Tepper and J. T. Mcleskey, Electrospun Polymer-Fiber Solar Cell, *Adv. Mater. Sci. Eng.*, 2013, 2013, 1–6, DOI: 10.1155/2013/975947.

- 3 A. M. Jordan, V. Viswanath, S.-E. Kim, J. K. Pokorski and L. T. J. Korley, Processing and Surface Modification of Polymer Nanofibers for Biological Scaffolds: A Review, *J. Mater. Chem. B*, 2016, 4(36), 5958–5974, DOI: 10.1039/C6TB01303A.
- 4 J. D. Hochberg, D. M. Wirth, G. Spiaggia, P. Shah, B. Rothen-Rutishauser, A. Petri-Fink and J. K. Pokorski, High-Throughput Manufacturing of Antibacterial Nanofibers by Melt Coextrusion and Post-Processing Surface-Initiated Atom Transfer Radical Polymerization, ACS Appl. Polym. Mater., 2022, 4(1), 260–269, DOI: 10.1021/acsapm.1c01264.
- 5 J. E. Oliveira, E. S. Medeiros, L. Cardozo, F. Voll, E. H. Madureira, L. H. C. Mattoso and O. B. G. Assis, Development of Poly(Lactic Acid) Nanostructured Membranes for the Controlled Delivery of Progesterone to Livestock Animals, *Mater. Sci. Eng.*, C, 2013, 33(2), 844–849, DOI: 10.1016/j.msec.2012.10.032.
- 6 S.-E. Kim, E. C. Harker, A. C. De Leon, R. C. Advincula and J. K. Pokorski, Coextruded, Aligned, and Gradient-Modified Poly(ε-Caprolactone) Fibers as Platforms for Neural Growth, *Biomacromolecules*, 2015, 16(3), 860–867, DOI: 10.1021/bm501767x.
- 7 S. Lyu, C. Huang, H. Yang and X. Zhang, Electrospun Fibers as a Scaffolding Platform for Bone Tissue, *Repair*, 2013, **8**, 1382–1389, DOI: **10.1002/jor.22367**.
- 8 L. A. Smith Callahan, S. Xie, I. A. Barker, J. Zheng, D. H. Reneker, A. P. Dove and M. L. Becker, Directed Differentiation and Neurite Extension of Mouse Embryonic Stem Cell on Aligned Poly(Lactide) Nanofibers Functionalized with YIGSR Peptide, *Biomaterials*, 2013, 34(36), 9089–9095, DOI: 10.1016/j.biomaterials.2013.08.028.
- 9 I. Esmaeilzadeh, V. Mottaghitalab, B. Tousifar, A. Afzali and M. Lamani, A Feasibility Study on Semi Industrial Nozzleless Electrospinning of Cellulose Nanofiber, *Int. J. Ind. Chem.*, 2015, 6(3), 193–211, DOI: 10.1007/s40090-015-0043-y.
- 10 A. Camerlo, A.-M. Bühlmann-Popa, C. Vebert-Nardin, R. M. Rossi and G. Fortunato, Environmentally Controlled Emulsion Electrospinning for the Encapsulation of Temperature-Sensitive Compounds, *J. Mater. Sci.*, 2014, 49(23), 8154–8162, DOI: 10.1007/s10853-014-8524-5.
- 11 N. Wang, K. Burugapalli, W. Song, J. Halls, F. Moussy, Y. Zheng, Y. Ma, Z. Wu and K. Li, Tailored Fibro-Porous Structure of Electrospun Polyurethane Membranes, Their Size-Dependent Properties and Trans-Membrane Glucose Diffusion, J. Membr. Sci., 2013, 427, 207–217, DOI: 10.1016/ j.memsci.2012.09.052.
- 12 F. Chen, G. Hochleitner, T. Woodfield, J. Groll, P. D. Dalton and B. G. Amsden, Additive Manufacturing of a Photo-Cross-Linkable Polymer via Direct Melt Electrospinning Writing for Producing High Strength Structures, *Biomacromolecules*, 2016, 17(1), 208–214, DOI: 10.1021/acs. biomac.5b01316.
- 13 F. Zuo, D. H. Tan, Z. Wang, S. Jeung, C. W. Macosko and F. S. Bates, Nanofibers from Melt Blown Fiber-in-Fiber

- Polymer Blends, *ACS Macro Lett.*, 2013, **2**(4), 301–305, DOI: **10.1021/mz400053n**.
- 14 M. R. Badrossamay, H. A. McIlwee, J. A. Goss and K. K. Parker, Nanofiber Assembly by Rotary Jet-Spinning, *Nano Lett.*, 2010, 10(6), 2257–2261, DOI: 10.1021/nl101355x.
- 15 M. R. Badrossamay, K. Balachandran, A. K. Capulli, H. M. Golecki, A. Agarwal, J. A. Goss, H. Kim, K. Shin and K. K. Parker, Engineering Hybrid Polymer-Protein Super-Aligned Nanofibers via Rotary Jet Spinning, *Biomaterials*, 2014, 35(10), 3188–3197, DOI: 10.1016/j.biomaterials.2013.12.072.
- 16 J. Wang, D. Langhe, M. Ponting, G. E. Wnek, L. T. J. Korley and E. Baer, Manufacturing of Polymer Continuous Nanofibers Using a Novel Co-Extrusion and Multiplication Technique, *Polymer*, 2014, 55(2), 673–685, DOI: 10.1016/j. polymer.2013.12.025.
- 17 S.-E. Kim, J. Wang, A. M. Jordan, L. T. J. Korley, E. Baer and J. K. Pokorski, Surface Modification of Melt Extruded Poly (ε-Caprolactone) Nanofibers: Toward a New Scalable Biomaterial Scaffold, *ACS Macro Lett.*, 2014, 3(6), 585–589, DOI: 10.1021/mz500112d.
- 18 A. M. Jordan and L. T. J. Korley, Toward a Tunable Fibrous Scaffold: Structural Development during Uniaxial Drawing of Coextruded Poly(ε-Caprolactone) Fibers, *Macromolecules*, 2015, 48(8), 2614–2627, DOI: 10.1021/acs.macromol.5b00370.
- 19 L. S. Nair and C. T. Laurencin, Biodegradable Polymers as Biomaterials, *Prog. Polym. Sci.*, 2007, 32(8-9), 762-798, DOI: 10.1016/j.progpolymsci.2007.05.017.
- 20 P. Gunatillake, R. Mayadunne and R. Adhikari. Recent Developments in Biodegradable Synthetic Polymers, in *Biotechnology Annual Review*, Elsevier, 2006, vol. 12, pp. 301–347. DOI: 10.1016/S1387-2656(06)12009-8.
- 21 B. Dhandayuthapani, Y. Yoshida, T. Maekawa and D. S. Kumar, Polymeric Scaffolds in Tissue Engineering Application: A Review, *Int. J. Polym. Sci.*, 2011, 2011, 1–19, DOI: 10.1155/2011/290602.
- 22 H. Sun and S. Önneby, Facile Polyester Surface Functionalization via Hydrolysis and Cell-Recognizing Peptide Attachment, *Polym. Int.*, 2006, 55(11), 1336–1340, DOI: 10.1002/pi.2090.
- 23 Y. Zhu, C. Gao, X. Liu and J. Shen, Surface Modification of Polycaprolactone Membrane via Aminolysis and Biomacromolecule Immobilization for Promoting Cytocompatibility of Human Endothelial Cells, Biomacromolecules, 2002, 3(6), 1312-1319, DOI: 10.1021/ bm020074v.
- 24 A.-D. Bendrea, L. Cianga, G.-L. Ailiesei, E.-L. Ursu, D. Göen Colak and I. Cianga, 3,4-Ethylenedioxythiophene (EDOT) End-Group Functionalized Poly-ε-Caprolactone (PCL): Self-Assembly in Organic Solvents and Its Coincidentally Observed Peculiar Behavior in Thin Film and Protonated Media, *Polymers*, 2021, 13(16), 2720, DOI: 10.3390/polym13162720.
- 25 C. Kósa, M. Sedlačík, A. Fiedlerová, Š. Chmela, K. Borská and J. Mosnáček, Photochemically Cross-Linked Poly(ε-

- Caprolactone) with Accelerated Hydrolytic Degradation, *Eur. Polym. J.*, 2015, **68**, 601–608, DOI: **10.1016/j.eurpolymj.2015.03.041**.
- 26 S.-E. Kim, C. Zhang, A. A. Advincula, E. Baer and J. K. Pokorski, Protein and Bacterial Antifouling Behavior of Melt-Coextruded Nanofiber Mats, ACS Appl. Mater. Interfaces, 2016, 8(14), 8928–8938, DOI: 10.1021/ acsami.6b00093.
- 27 M. Li, M. Fromel, D. Ranaweera, S. Rocha, C. Boyer and C. W. Pester, SI-PET-RAFT: Surface-Initiated Photoinduced Electron Transfer-Reversible Addition-Fragmentation Chain Transfer Polymerization, *ACS Macro Lett.*, 2019, **8**(4), 374–380, DOI: **10.1021/acsmacrolett.9b00089**.
- 28 S. Shanmugam, J. Xu and C. Boyer, Exploiting Metalloporphyrins for Selective Living Radical Polymerization Tunable over Visible Wavelengths, *J. Am. Chem. Soc.*, 2015, 137(28), 9174–9185, DOI: 10.1021/jacs.5b05274.
- 29 G. Ng, J. Yeow, J. Xu and C. Boyer, Application of Oxygen Tolerant PET-RAFT to Polymerization-Induced Self-Assembly, *Polym. Chem.*, 2017, 8(18), 2841–2851, DOI: 10.1039/C7PY00442G.
- 30 S.-E. Kim, A. M. Jordan, L. T. J. Korley and J. K. Pokorski, Drawing in Poly(ε-Caprolactone) Fibers: Tuning Mechanics, Fiber Dimensions and Surface-Modification Density, *J. Mater. Chem. B*, 2017, 5(23), 4499–4506, DOI: 10.1039/C7TB00096K.
- 31 B. Neises and W. Steglich, Simple Method for the Esterification of Carboxylic Acids, *Angew. Chem., Int. Ed. Engl.*, 1978, 17(7), 522–524, DOI: 10.1002/anie.197805221.
- 32 M. A. Woodruff and D. W. Hutmacher, The Return of a Forgotten Polymer—Polycaprolactone in the 21st Century, *Prog. Polym. Sci.*, 2010, 35(10), 1217–1256, DOI: 10.1016/j. progpolymsci.2010.04.002.
- 33 J. Pal, N. Kankariya, S. Sanwaria, B. Nandan and R. K. Srivastava, Control on Molecular Weight Reduction of Poly(ε-Caprolactone) during Melt Spinning—A Way to Produce High Strength Biodegradable Fibers, *Mater. Sci. Eng.*, C, 2013, 33(7), 4213–4220, DOI: 10.1016/j. msec.2013.06.011.
- 34 K. Agarwal, A. Sharma and G. Talukder, Effects of Copper on Mammalian Cell Components, *Chem.-Biol. Interact.*, 1989, 69(1), 1–16, DOI: 10.1016/0009-2797(89)90094-X.
- 35 J. Li, H. Yun, Y. Gong, N. Zhao and X. Zhang, Investigation of MC3T3-E1 Cell Behavior on the Surface of GRGDS-Coupled Chitosan, *Biomacromolecules*, 2006, 7(4), 1112–1123, DOI: 10.1021/bm050913r.
- 36 U. Hersel, C. Dahmen and H. Kessler, RGD Modified Polymers: Biomaterials for Stimulated Cell Adhesion and Beyond, *Biomaterials*, 2003, 24(24), 4385–4415, DOI: 10.1016/S0142-9612(03)00343-0.
- 37 S. L. Bellis, Advantages of RGD Peptides for Directing Cell Association with Biomaterials, *Biomaterials*, 2011, 32(18), 4205–4210, DOI: 10.1016/j.biomaterials.2011.02.029.